

Quantum electrodynamics and plasmonic resonance of metallic nanostructures

This content has been downloaded from IOPscience. Please scroll down to see the full text.

2016 J. Phys.: Condens. Matter 28 155302

(<http://iopscience.iop.org/0953-8984/28/15/155302>)

View [the table of contents for this issue](#), or go to the [journal homepage](#) for more

Download details:

This content was downloaded by: mingliangster

IP Address: 130.166.120.137

This content was downloaded on 21/03/2016 at 17:59

Please note that [terms and conditions apply](#).

Quantum electrodynamics and plasmonic resonance of metallic nanostructures

Mingliang Zhang, Hongping Xiang, Xu Zhang and Gang Lu

Department of Physics and Astronomy, California State University Northridge, Northridge, CA 91330, USA

E-mail: ganglu@csun.edu

Received 21 October 2015, revised 22 February 2016

Accepted for publication 23 February 2016

Published 17 March 2016



Abstract

Plasmonic resonance of a metallic nanostructure results from coherent motion of its conduction electrons driven by incident light. At the resonance, the induced dipole in the nanostructure is proportional to the number of the conduction electrons, hence 10^7 times larger than that in an atom. The interaction energy between the induced dipole and fluctuating virtual field of the incident light can reach a few tenths of an eV. Therefore, the classical electromagnetism dominating the field may become inadequate. We propose that quantum electrodynamics (QED) may be used as a fundamental theory to describe the interaction between the virtual field and the oscillating electrons. Based on QED, we derive analytic expressions for the plasmon resonant frequency, which depends on three easily accessible material parameters. The analytic theory reproduces very well the experimental data, and can be used in rational design of materials for plasmonic applications.

Keywords: localized surface plasmonic resonance frequency, red shift, vacuum virtual electromagnetic field, lamb shift, shape and size dependence

 Online supplementary data available from stacks.iop.org/JPhysCM/28/155302/mmedia

(Some figures may appear in colour only in the online journal)

When light interacts with a metallic nanostructure, its conduction electrons may undergo collective oscillations driven by the electric field of the light. Known as localized surface plasmon resonance (LSPR), the collective oscillations can be tuned by adjusting the shape, size and surrounding medium of the nanostructure, which is at the heart of the burgeoning field of plasmonics with potential applications ranging from photocatalysis [1, 2] to optics, chemical and biological sensing [3], and photo-thermal therapeutics, to name a few [4–8].

Although the fundamental physical theory of light-matter interaction is quantum electrodynamics (QED) [9, 10], traditionally, QED has not been brought to bear on problems in plasmonics. The present research paradigm of plasmonics is rooted in classical electrodynamics where the electromagnetic field of the light is treated classically. It is generally believed that QED correction is too small to be relevant in practical plasmonic applications. The tremendous success of the classical theory has certainly reinforced this notion. However, as we will show in this paper that the QED correction cannot

be ignored in plasmonic resonance. In fact, for collective excitations such as LSPR, the QED correction could result in an energy shift on the order of a few tenths of an eV, well within the range of experimental probes. For nanoparticles, neglecting the correction would lead to a size-dependence of resonant frequency that is contradictory to experiments. The main purpose of the paper is to highlight the importance and elucidate the consequence of QED in plasmonics. Focusing on plasmonic resonance of metallic nanostructures, we illustrate the origin of the plasmonic energy shift and derive analytic expressions for the resonant frequency. The theory is compared to available experimental results on nano-spheres, nano-rods and nano-plates and shows promise as a rapid means for screening materials and structures in plasmonic applications.

The present theory of plasmonic resonance rests on a classical description of the electromagnetic field, irrespective of whether the electrons are treated quantum mechanically or not [11–13]. In QED, the electromagnetic field is quantized and there exists a virtual fluctuating electromagnetic field in

vacuum carrying zero-point energy. The fluctuating virtual field results in a fluctuation of electronic coordinates, leading to a change in the Coulomb energy between the electrons and the positive ions. This energy change owing to the virtual electromagnetic field is known as Lamb shift in atomic physics, and usually extremely small [10]. In a typical plasmonic nanostructure, the wavelength of the visible light, the beam width and the skin-depth are all greater than the size of the nanostructure [14, 15], hence *all* conduction electrons in the nanostructure undergo coherent and collective oscillations. The higher energy oscillations are longitudinal, corresponding to so-called ‘bulk’ plasmon, while the lower energy oscillations are transverse and correspond to the LSPR [16]. All electrons are involved in both modes of oscillations. For a nanoparticle of a radius of 100 nm, the coherent oscillation could involve $\sim 10^7$ conduction electrons, leading to an induced dipole moment that is 6–7 orders of magnitude stronger than that in an atom. Since the interaction energy of the fluctuating virtual field with the conduction electrons is proportional to the induced dipole, the energy shift can reach several tenths of an eV, which can be measured experimentally.

Let H_e be the electronic Hamiltonian of the nanostructure, and $\{|a\rangle, |b\rangle, \dots\}$ and $\{E_a, E_b, \dots\}$ as the eigenstates and eigenvalues of H_e , respectively. Let H_f be the Hamiltonian of the incident electromagnetic field including both the external field and the virtual field. The eigenstates of H_f are labeled as $|n_{\mathbf{k}_1\mathbf{e}_1}, n_{\mathbf{k}_2\mathbf{e}_2}, \dots\rangle$, where $n_{\mathbf{k}_i\mathbf{e}_i}$ is the occupation number in the photon state $\mathbf{k}_i\mathbf{e}_i$ (\mathbf{k}_i is the wave-vector and \mathbf{e}_i is the polarization vector). The total Hamiltonian of the system is thus

$$H = (H_e + H_f) + U, \quad (1)$$

where U is the interaction between the conduction electrons and the virtual field. Since the wavelength of the field is much larger than the size of the nanostructure, the interaction energy U can be expressed as [9, 10]

$$U = - \sum_j \hat{\mathbf{d}}_j \cdot \mathbf{E}(\mathbf{r}_j), \quad (2)$$

where $\mathbf{E}(\mathbf{r}_j)$ is the electric field at position \mathbf{r}_j of the j th electron, and $\hat{\mathbf{d}}_j$ is the dipole operator of the j th electron. The extinction spectrum of the nanostructure, comprised of the absorption and scattering spectrum of the incident photon, is the primary physical quantity that can be measured experimentally and calculated theoretically. According to QED [9, 17], the resonant frequency ω_{res} of the extinction spectrum consists of two contributions:

$$\omega_{\text{res}} = \omega_m + \Delta. \quad (3)$$

$\hbar\omega_m$ represents the excitation energy of the plasmons. Since the plasmons or the coherent oscillations are the eigenstates of H_e , denoted by Ψ_m , ω_m is the corresponding eigenfrequency. Δ is the frequency shift resulted from the interaction of the electrons with the virtual field.

Here we derive an analytical expression for this eigenfrequency, with the oscillations along one of the major axes of the nanostructure. To a good approximation, nanostructures such as spheres, rods, and circular plates can be modeled as ellipsoids with a uniform volume polarization.

Suppose that a metallic ellipsoid with a dielectric function $\varepsilon_1 = \varepsilon_1' + i\varepsilon_1''$ is embedded in a medium with a dielectric function $\varepsilon_2 = \varepsilon_2' + i\varepsilon_2''$, and the electric field of the incident photon, E_z^{ext} , is along the z -axis of the ellipsoid. If the longest dimension the ellipsoid, L_{max} , is much smaller than $\lambda\varepsilon_2'^{-1/2}/4$ (λ is the wavelength), the beam width W of the incident light [14], and the skin-depth $\delta = \lambda(2\pi\varepsilon_1''^{1/2})^{-1}$, the quasi-static approximation is valid [15]. The quasi-static approximation implies the phase change across the nanostructure should be small, i.e. $2\pi L_{\text{max}}/(\lambda\varepsilon_2'^{-1/2}) \ll \pi/2$. For the violet light with $\lambda = 4000 \text{ \AA}$ in vacuum ($\varepsilon_2' = 1$), one arrives at $L_{\text{max}} < 100 \text{ nm}$. The phase retardation effect can be observed when the particle size is larger than 20 nm, and becomes important when $L_{\text{max}} \gtrsim 100 \text{ nm}$. Under the quasi-static approximation, the total induced dipole moment in the ellipsoid is given by [15, 16]:

$$\mathcal{P}_{1z} = \alpha_z V \varepsilon_0 E_z^{\text{ext}}, \quad \text{with } \alpha_z = \frac{\varepsilon_2(\varepsilon_1 - 1)}{\varepsilon_2 + (\varepsilon_1 - \varepsilon_2)n^{(z)}}. \quad (4)$$

Here V is the volume of the ellipsoid; ε_0 is the permeability of free space and $n^{(z)}$ is the depolarization factor along the z -axis. Note that equation (4) corresponds to $(\pi L_{\text{max}} \varepsilon_2'^{1/2}/\lambda)^3$ terms in the Mie theory [16]. To capture the phase retardation effect in larger nanostructures ($L_{\text{max}} > 100 \text{ nm}$), one can include the higher terms such as $(\pi L_{\text{max}} \varepsilon_2'^{1/2}/\lambda)^5$ in the Mie theory, which correspond to the induced electric quadrupole and magnetic dipole of the nanostructure [15]. We now make two assumptions: (1) ε_2' is a constant, which is a reasonable assumption for commonly used media, such as vacuum, SiO_2 and polyvinyl alcohol, in plasmonic applications. (2) The dielectric functions of the nanostructures are primarily determined by the conduction electrons [18], which is also a reasonable approximation. Under these assumptions, the dielectric functions of the nanostructure can be expressed as:

$$\varepsilon_1' = 1 - \frac{S\omega_p^2}{\omega^2 + \gamma^2}, \quad \varepsilon_1'' = \frac{S\gamma\omega_p^2}{\omega^3 + \gamma^2\omega}. \quad (5)$$

Here $\omega_p = (ne^2/m\varepsilon_0)^{1/2}$ is the plasmon frequency. n and m denote the electron number density and mass of the electron. $S(\omega)$ represents intra-band oscillator strength of the conduction electrons. γ is the decay rate of the quasiparticles, given by [18–21]:

$$\gamma = \gamma_0 + A v_F / L_{\text{eff}}, \quad (6)$$

where $v_F = \hbar(3\pi^2 n)^{1/3}/m$ is the Fermi velocity of the metal and L_{eff} is the effective dimension of the ellipsoid along the polarization direction. A is a dimensionless, positive constant on the order of one. γ_0 is the decay rate resulting from electron–phonon, electron–impurity, and electron–electron interactions [18], and can be estimated by $\gamma_0 = ne^2/m\sigma$ with σ as the conductivity of the metal. The second term in equation (6) stems from electron scattering with the surface, and is the only term dependent on the size of the nanostructure.

Note that the derivation of equation (5) is based the free electron model where the wave-functions of the single particle states are Bloch waves. On the other hand, if the shortest dimension of the metallic nanostructure, L_{min} , is small, the corresponding

wave-functions are best described standing waves. To ensure that the wave-vectors at the Brillouin zone boundary have an acceptable error ($< 10\%$), L_{\min} has to be greater than 2 nm. Therefore, our analytical results are valid in the size range of $2 \text{ nm} < L < 100 \text{ nm}$. In the classical electromagnetism, the extinction cross-section $\sigma_{\text{ex}}^c(\omega)$ of the nanostructure is [15] proportional to $\{[\varepsilon_2' + (\varepsilon_1' - \varepsilon_2')n^{(z)}]^2 + [\varepsilon_2'' + (\varepsilon_1'' - \varepsilon_2'')n^{(z)}]^2\}^{-1}$. We show in the supplementary information (stacks.iop.org/JPhysCM/28/155302/mmedia) that the eigenfrequency ω_m maximizes $\sigma_{\text{ex}}^c(\omega)$. Therefore ω_m is the root of the following equation [22–31]:

$$\varepsilon_2' + (\varepsilon_1' - \varepsilon_2')n^{(z)} = 0. \quad (7)$$

Equation (7) yields the expression for the eigenfrequency ω_m :

$$\omega_m = \omega_p \left[\frac{S}{1 + \varepsilon_2' \left(\frac{1}{n} - 1 \right)} - \left(\frac{\gamma}{\omega_p} \right)^2 \right]^{1/2}. \quad (8)$$

Here and later we drop the superscript z for brevity when there is no confusion.

Based on non-perturbative many-body quantum theory, the frequency shift Δ can be determined from the Green's function of the Hamiltonian (1). Specifically, $\hbar\Delta = \text{Re}(R)$ and R is the shift-operator of the Green's function, given by [9]

$$R = \sum_{a\mathbf{k}\mathbf{e}} \frac{|\langle a; \mathbf{k}\mathbf{e} | U | \Psi_m; 0 \rangle|^2}{E_m - E_a - \hbar\omega_{\mathbf{k}\mathbf{e}}} + \sum_{a\mathbf{k}\mathbf{e}} \sum_{a'\mathbf{k}'\mathbf{e}'} \quad (9)$$

$$\frac{\langle \Psi_m; 0 | U | a; \mathbf{k}\mathbf{e} \rangle \langle a; \mathbf{k}\mathbf{e} | U | a'; \mathbf{k}'\mathbf{e}' \rangle \langle a'; \mathbf{k}'\mathbf{e}' | U | \Psi_m; 0 \rangle}{(E_m - E_a - \hbar\omega_{\mathbf{k}\mathbf{e}})(E_m - E_{a'} - \hbar\omega_{\mathbf{k}'\mathbf{e}'})} + \dots,$$

where E_m is the energy of the eigenstate Ψ_m ; $|\Psi_m; 0\rangle$ represents the many-body state at which the incident photon is absorbed and the plasmon is excited. $|a; \mathbf{k}\mathbf{e}\rangle$ denotes direct-product state of a many-electron state $|a\rangle$ and a virtual photon state with a wave-vector \mathbf{k} and a polarization vector \mathbf{e} . Finally, we arrive at

$$\Delta = -\frac{\omega_m}{4} \frac{\beta_z}{1 + \beta_z}, \quad (10)$$

with

$$\beta_z = \frac{V}{\lambda_m^3} \frac{\varepsilon_2'^2}{[n^{(z)}]^2} \left\{ 1 + \left(\frac{\varepsilon_1' - 1}{\varepsilon_1''} \right)^2 \right\}. \quad (11)$$

Here $\lambda_m = 2\pi c/\omega_m$. In equation (11), ε_1' and ε_1'' are evaluated at $\omega = \omega_m$. As $\beta_z \geq 0$, the frequency shift Δ is less than $1/4$ of ω_m . The central aim of this work is to demonstrate that the interaction of the induced dipole and the vacuum fluctuation of the electromagnetic field causes a red shift Δ of the resonance frequency with increasing the volume of a nanostructure. The equations (7), (10) and (11) are valid for arbitrary dielectric functions. Using Drude model, we have derived an analytical expression for the dielectric functions in equation (5) and ultimately a simple analytical expression for ω_m in equation (8). However, one should bear in mind that the Drude model is only valid for free-electron like metals, such as Na. For noble metals such as Ag and Au, only low-energy plasmonic excitations involving s -electrons can be described correctly by the Drude model. We find that

for the energy range ($< 3.5 \text{ eV}$) examined in this paper, the s -electrons dominate the plasmonic excitations in Ag and Au, and thus the Drude model is appropriate. According to equations (8) and (10), there are three contributions to ω_{res} . Among them, the dominant one is the first term in equation (8) since $\frac{\gamma}{\omega_p} \ll 1$; the second term in equation (8) is the smallest among them. The dominant term depends *only* on the shape of the nanostructure through the depolarization factor, $n^{(z)}$. Hence the resonant frequency ω_{res} of the nanostructure is determined primarily by its shape as opposed to its size. This fact has been well established and exploited in plasmonics [22, 23]. More importantly, γ in equation (8) is a monotonically decreasing function of L_{eff} as indicated in equation (6), hence ω_m is a weakly increasing function of the particle size. If there were no correction term Δ , the resonant frequency ω_{res} ($=\omega_m$) would have been a monotonically increasing function of the particle size, which is opposite to the experimental observations [21, 24, 25, 30]. The QED correction term, Δ , as a decreasing function of the particle size, reverses the incorrect size-dependence of the classical electromagnetic theory and renders ω_{res} consistent with the experiments. The failure of the classical theory has also been discussed by Scholl *et al* [25] who attributed the opposite size-dependence to the inappropriate use of macroscopic dielectric functions in the nanoparticles. The macroscopic dielectric functions failed to capture the effects of discrete energy levels and the fact that only certain electronic or plasmonic transitions are allowed in the nanoparticles. To remedy the classical theory, Scholl *et al* proposed a phenomenological model based on discrete energy levels. Although the model yielded an improved agreement to the experimental data, it did not consider the quantum effect of the electromagnetic field. As a result, the model cannot guarantee the *monotonically* decreasing size-dependence of ω_{res} , as revealed in experiments and the present theory. Nonetheless, Scholl's model is a valuable contribution and could be combined with the present theory to form a more comprehensive microscopic picture of plasmonic resonance.

If the electric field of the incident light is perpendicular to the z -axis, the depolarization factor in the normal direction has to be worked out. We have derived the corresponding equations, which are included in the supplementary information. Moreover, if the electric field of the incident light is along an arbitrary direction, the total induced dipole is a vector sum of the components in each major axis [15, 16]. Finally, for a spheroid with its rotational axis along z , the depolarization factors $n^{(x)}$, $n^{(y)}$, $n^{(z)}$ and the resonant frequency $\omega_{\text{res}}^{\parallel}(\mathbf{E}_{\text{ext}} \parallel z)$ and $\omega_{\text{res}}^{\perp}(\mathbf{E}_{\text{ext}} \perp z)$ can be calculated analytically as well. For a general ellipsoid, the corresponding quantities have to be evaluated numerically.

The size dependence of plasmonic resonance frequency in metallic nanostructures has been studied extensively and several physical origins have been proposed, including size-dependent dielectric functions [25, 32, 33], phase retardation [34, 35], and nonlocal response of current to the electromagnetic field [36–43], etc. However, in all previous works, the electromagnetic field was treated classically.

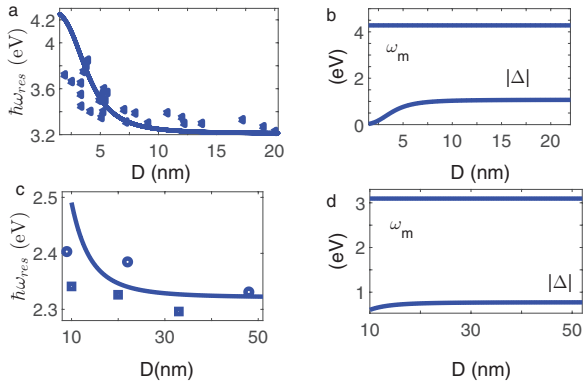


Figure 1. (a) and (c) The plasmon resonant energy $\hbar\omega_{\text{res}}$ as a function of the nano-sphere diameter D , compared between the theory (solid curve) and experimental data (symbols). The triangles in (a) are from the experiment [25] for Ag and the circles and squares in (c) are from [30] and [31] for Au, respectively. (b) and (d) The contribution of ω_m and $|\Delta|$ as a function of D for Ag and Au, respectively.

To validate the proposed theory, we apply it to various metallic nanostructures including nano-spheres, nano-rods, and nano-plates. First, we examine the size-dependence of ω_{res} in nano-spheres. Since all spheres have the same shape or the depolarization factors [15] ($n = 1/3$), the nano-spheres of the same metal would yield the same ω_m for a given surrounding medium. According to equations (10) and (11), Δ depends only on the volume of a sphere, thus ω_{res} is a monotonically decreasing function of the sphere diameter D . When comparing to experimental results for nanoparticles, one should be cautious. This is because in most experiments where plasmon resonance of nanoparticles is measured, the nanoparticles are often covered by ligands. Since the ligands tend to attract electrons from the nanoparticles, the measured resonant energies may deviate considerably from their intrinsic values, for which the theoretical model is developed. More importantly, nanoparticles with different sizes are affected differently by the ligands (the smaller the particle, the greater the effect), thus yielding different size-dependence of the resonance energy. To avoid this problem, we choose to focus on experiments where the nanoparticles are ligand-free. One such experiment which has attracted a lot attention is the work of Scholl *et al* [25] who have measured the plasmon resonance of individual ligand-free Ag nanoparticles using aberration-corrected transmission electron microscope (TEM) and mono-chromated scanning TEM electron energy-loss spectroscopy. In figure 1(a), we compare the theoretical prediction to the experimental data taken from figure 3(b) of Scholl's paper [25]. The dielectric constant of the surrounding medium ϵ'_2 is 1.69 as measured in the experiment. We find that the theoretical prediction agrees very well to the experimental data as long as the two fitting parameters A and S are chosen reasonably, in this case $A = 0.03$, $S = 1$. It is important to point out that the present theory predicts the correct experimental trend—a *monotonic* redshift as D increases, regardless the choice of A and S . As displayed in figure 1(b), the size dependence of ω_{res} is entirely contained in Δ while ω_m is essentially flat. Thus the size-dependence of the nano-spheres originates exclusively from

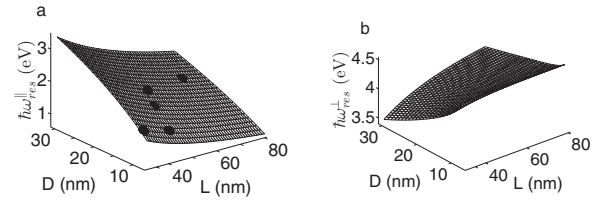


Figure 2. The plasmonic resonance energy of a Au nano-rod embedded in SiO_2 as a function of its diameter D and length L , compared between the theory (surface) and experiment (dots). The polarization direction is parallel (a) and perpendicular (b) to the nano-rod long-axis.

the quantum nature of the electromagnetic field. To the best of our knowledge, the present theory is the only one that yields the correct experimental trend for ligand-free nanoparticles in the range between 2 nm and 20 nm. For Ag *nanowires*, self-consistent hydrodynamic model reproduced the same trend as in Scholl's work on Ag *nanoparticles* [44]. However, for Na nanowires, the same method predicted a redshift first then a blueshift as the nanowire radius increases. For Na nanoparticles, the quantum mechanical time-dependent orbital-free density functional theory (TD-OFDFT) calculations reported a redshift first, then a blueshift and then a redshift again as the particle diameter varies from 1 nm to 12 nm [45]. The time-dependent DFT calculations reported a blueshift for small particles less than 2 nm [46] for Ag nanoparticles. It is important to point out, however, that the electric quadrupole, magnetic dipole and phase retardation can also lead to the redshift, but for much larger particles (>100 nm) [16]. Similar comparison is made for gold nano-spheres embedded in water whose dielectric constant $\epsilon'_2 = 1.78$. As shown in figures 1(c) and (d), the fitting parameters are $A = 0.01$, $S = 0.54$.

Second, we compare the theoretical prediction to the experimental results for Au nano-rods embedded in silica [23] ($\epsilon'_2 = 2.15$). In figure 2(a), the experimental resonance frequency $\omega_{\text{res}}^{\parallel}$ as function of the length L and diameter D of the nano-rods is shown in circles, while the theoretical prediction is on the surface. In this case, the two fitting parameters are $A = 0.6$, $S = 1.4$. Because L is ~ 32 – 70 nm [23], larger than the size of the nano-spheres, the electron scattering at the surface becomes more important, thus A is larger. For the similar reason, the oscillator strength S is also larger than the nano-spheres, as discussed in the supplementary information. There is an overall good agreement between the theory and experiment, down to the size of 8.5 nm [23]. The theoretical prediction for the polarization direction perpendicular to the nano-rod axis is displayed in figure 2(b).

We next demonstrate the validity of ω_m , which cannot be measured directly by experiments. Hence, we compare the theoretical prediction of ω_m to a set of computational results obtained from TD-OFDFT simulations [45, 47] for a Na nano-rod embedded in vacuum ($\epsilon'_2 = 1$). A number of (L, D) combinations including (5.79, 0.86), (5.79, 1.41), (5.79, 1.93), (5.79, 2.23), (5.79, 3.54), (5.79, 4.76), and (5.79, 5.46), in the unit of nm, are considered. The two fitting parameters are $A = 0.6$, $S = 0.8$ for $\mathbf{E} \parallel$ axis and $A = 0.6$, $S = 0.92$ for $\mathbf{E} \perp$ axis. There is an excellent agreement between the theoretical

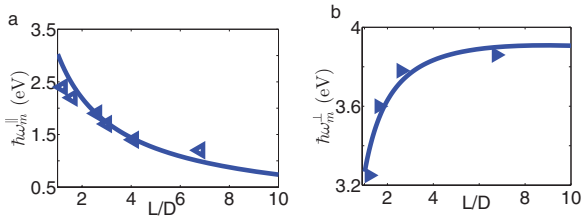


Figure 3. The eigenfrequency ω_m as a function of L/D for a Na nano-rod in vacuum, determined from the theory (curve) and the TD-OFDFT calculations (triangles). The polarization direction is parallel (a) and perpendicular (b) to the nano-rod long-axis.

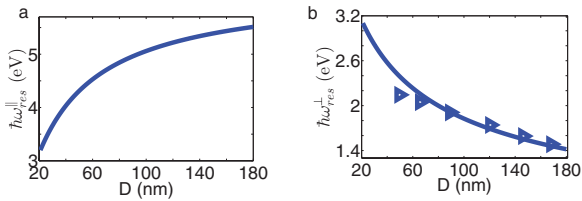


Figure 4. The plasmonic resonance energy as a function of diameter D for a circular gold nano-plate with a fixed height $L = 20$ nm. The results from theory are shown in solid curves while the experimental data is shown as triangles; the polarization direction is parallel (a) and perpendicular (b) to the long-axis of the plate.

predictions and the TD-OFDFT results for both polarization directions as shown in figure 3, which validates the derivation of ω_m . In figures 2 and 3, one may notice that $\hbar\omega_{\text{res}}^{\parallel}(L, D)$ has an opposite size-dependence as $\hbar\omega_{\text{res}}^{\perp}(L, D)$, owing to the opposite (L, D) dependence of $n^{(z)}$ and $n^{(x)}$.

Third, we switch to a Au nano-plate whose rotational symmetric axis is along z . The theoretical predictions for $\omega_{\text{res}}^{\perp}(D)$ are compared to the experimental results [22]. The circular nano-plate has a height $L = 20$ nm embedded in a medium with a refractive index of 1.26. The fitting parameters $A = 0.6$, $S = 0.86$ yield an excellent agreement between the theoretical predictions and the experimental data as shown in figure 4. Similar agreement between the theory and experiments is also observed for Al and Pt nano-plates which is presented in the supplementary information. The opposite D -dependence between $\omega_{\text{res}}^{\parallel}(D)$ and $\omega_{\text{res}}^{\perp}(D)$ is due to the opposite D -dependence of their respective depolarization factors.

Although size-dependent dielectric functions could be invoked to explain the size-dependence of ω_{res} , such explanation is restricted to small nanoparticles. One can estimate the maximum radius R of the nanoparticles above which the size-dependent dielectric functions become indistinguishable from the bulk dielectric functions. It is known that the presence of discrete energy levels is the origin of the size-dependent dielectric functions [25]. Hence if the level spacing becomes comparable or smaller than $\hbar\gamma_0$ ($\gamma_0 = v_F/l$ where l is the mean free path of bulk material), the dielectric functions are no longer size-dependent. This condition leads to $R \sim \pi(\hbar/8mv_F)^{1/2}$. Taking $l \sim 10^3$ Å, $v_F \sim 3 \times 10^6$ m s⁻¹, we have $R \sim 2.2$ nm. Clearly, for the size range $2 < L_{\text{max}} < 100$ nm discussed in this work, the size-dependence of ω_{res} cannot be described by the size-dependent dielectric functions.

The QED formalism provides a plausible framework whose predictions agree well with the experimental observations. QED could have more profound implications in plasmonics than what is presented in this paper. For example, it is known that when a nano-antenna is placed next to a metallic nanostructure, there is an interaction between the nano-antenna (an emitter) and the virtual field. The interaction could change the directional radiation pattern of the antenna [48], analogous to cavity QED [49]. The present work, on the other hand, focuses on the interaction between an absorber (the plasmonic nanostructure) and the virtual field. Such interaction could also change the induced magnetic moment of the metallic nanostructure, as well as the polarization of the incident light.

To summarize, we propose that QED is important to understand the plasmonic resonance in metallic nanostructures, specially nanoparticles. The coherent motion of the conduction electrons in the nanostructure could lead to a large induced dipole moment, which interacts with the virtual field and results in a significant shift in the resonant frequency. The frequency shift is the key to reconciling the theoretical predictions and experimental observations on size-dependent plasmonic resonance. Based on QED, we have derived analytic expressions for the plasmonic resonant frequency, which depends on three easily accessible material parameters—the dielectric constant ϵ'_2 of the surrounding medium, the number density n of electrons and the conductivity σ of the metal. The analytic expression are shown to reproduce very well the experimental data for nano-spheres, nano-rods and nano-plates, and can be used readily for estimating the resonant frequency of plasmonic nanostructures as a function of their geometry, composition and surrounding medium.

Acknowledgment

The work was supported by an Army Research Office grant W911NF-12-1-0072 and NSF PREM Grant (DMR-1205734).

References

- [1] Mukherjee S, Libisch F, Large N, Neumann O, Brown L V, Cheng J, Lassiter J B, Carter E A, Nordlander P and Halas N J 2013 Hot electrons do the impossible: plasmon-induced dissociation of H₂ on Au *Nano Lett.* **13** 240–7
- [2] Linic S, Aslam U, Boerigter C and Morabito M 2015 Photochemical transformations on plasmonic metal nanoparticles *Nat. Mater.* **14** 567–76
- [3] Mayer K M and Hafner J H 2011 Localized surface plasmon resonance sensors *Chem. Rev.* **111** 3828–57
- [4] Halperin W P 1986 Quantum size effects in metal particles *Rev. Mod. Phys.* **58** 533–606
- [5] Link S and El-Sayed M A 2003 Optical properties and ultrafast dynamics of metallic nanocrystals *Annu. Rev. Phys. Chem.* **54** 331–66
- [6] Kalsin A, Fialkowski M, Paszewski M, Smoukov S K, Bishop K J M, Grzybowski B A 2006 Electrostatic self-assembly of binary nanoparticle crystals with a diamond-like lattice *Science* **312** 420–4
- [7] Stuart D A, Yuen J M, Shah N, Lyandres O, Yonzon C R, Glucksberg M R, Walsh J T, Duyne P V 2006 In vivo glucose measurement by surface-enhanced Raman spectroscopy *Anal. Chem.* **78** 7211–15

- [8] Huang X, El-Sayed I H, Qian W, El-Sayed M A 2006 Cancer cell imaging and photothermal therapy in the near-infrared region by using gold nanorods *J. Am. Chem. Soc.* **128** 2115–20
- [9] Cohen-Tannoudji C, Dupont-Roc J and Grynberg G 1992 *Atom—Photon Interactions: Basic Process and Applications* (New York: Wiley)
- [10] Berestetskii V B, Lifshitz E M and Pitaevskii L P 1982 *Quantum Electrodynamics* (Boston: Butterworth-Heinemann)
- [11] Kulkarni V, Prodan E and Nordlander P 2013 Quantum plasmonics: optical properties of a nanomatryushka *Nano Lett.* **13** 5873
- [12] Song P, Meng S, Nordlander P and Gao S 2012 Quantum plasmonics: symmetry-dependent plasmon-molecule coupling and quantized photoconductances *Phys. Rev. B* **86** 121410
- [13] Morton S M, Silverstein D W and Jensen L 2011 Theoretical studies of plasmonics using electronic structure theory *Chem. Rev.* **111** 3962–94
- [14] Crawford F S 1968 *Waves* (New York: McGraw-Hill)
- [15] Landau L D, Lifshitz E M and Pitaevskii L P 1984 *Electrodynamics of Continuous Media* 2nd edn (Amsterdam: Butterworth)
- [16] Stratton J A 1941 *Electromagnetic Theory* (New York: McGraw-Hill)
- [17] Bruun G M, Jackson A D and Kolomeitsev E E 2005 Multichannel scattering and feshbach resonances: effective theory, phenomenology, and many-body effects *Phys. Rev. A* **71** 052713
- [18] Callaway J 1991 *Quantum Theory of the Solid State* 2nd edn (Boston: Academic)
- [19] Lee K-S and El-Sayed M A 2005 Dependence of the enhanced optical scattering efficiency relative to that of absorption for gold metal nanorods on aspect ratio, size, end-cap shape, and medium refractive index *J. Phys. Chem B* **109** 20331–8
- [20] Coronado E A and Schatz G C 2003 Surface plasmon broadening for arbitrary shape nanoparticles: a geometrical probability approach *J. Chem. Phys.* **119** 3926–34
- [21] Jain P K, Lee K S, El-Sayed I H and El-Sayed M A 2006 Calculated absorption and scattering properties of gold nanoparticles of different size, shape, and composition: applications in biological imaging and biomedicine *J. Phys. Chem. B* **110** 7238–48
- [22] Zorić I, Zäch M, Kasemo B and Langhammer C 2011 Gold, platinum, and aluminum nanodisk plasmons: material independence, subradiance, and damping mechanisms *ACS Nano* **3** 2535–46
- [23] Juvé V, Cardinal M F, Lombardi A, Crut A, Maioli P, Perez-Juste J, Liz-Marzan L M, Fatti N D and Vallée F 2013 Size-dependent surface plasmon resonance broadening in nonspherical nanoparticles: single gold nanorods *Nano Lett.* **13** 2234–40
- [24] Baida H et al 2009 Quantitative determination of the size dependence of surface plasmon resonance damping in single Ag@SiO₂ nanoparticles *Nano Lett.* **9** 3463–69
- [25] Scholl J A, Koh A L and Dionne J A 2012 Quantum plasmon resonances of individual metallic nanoparticles *Nature* **483** 421–7
- [26] Klar T, Perner M, Grosse S, von Plessen G, Spirkl W and Feldmann J 1998 Surface-plasmon resonances in single metallic nanoparticles *Phys. Rev. Lett.* **80** 4249–52
- [27] Voisin C, Fatti N D, Christofilos D and Vallée F 2001 Ultrafast electron dynamics and optical nonlinearities in metal nanoparticles *J. Phys. Chem. B* **105** 2264–80
- [28] Kreibig U 1976 Small silver particles in photosensitive glass *Appl. Phys.* **10** 255–64
- [29] Noguez C 2007 *J. Phys. Chem. C* **111** 3806–19
- [30] Link S and El-Sayed M A 1999 Size and temperature dependence of the plasmon absorption of colloidal gold nanoparticles *J. Phys. Chem. B* **103** 4212–7
- [31] Berciaud S, Cognet L, Tamarat P and Lounis B 2005 Observation of intrinsic size effects in the optical response of individual gold nanoparticles *Nano Lett.* **5** 515–8
- [32] Ringe E, Zhang J, Langille M R, Sohn K, Cobley C, Au L, Xia Y, Mirkin C A, Huang J, Marks L D and Van Duyne R P 2010 *Mater. Res. Soc. Symp. Proc.* **1208** O10–02
- [33] Losurdo M, Giangreorio M M, Bianco G V, Suvorova A A, Kong C, Rubanov S, Capezzuto P, Humlicek J and Bruno G 2010 *Phys. Rev. B* **82** 155451
- [34] Davis T J, Vernon K C and Gómez D E 2009 *Opt. Express* **17** 23655–63
- [35] Lecarme O, Sun Q, Ueno K and Missawa H 2014 *ACS Photonics* **1** 538
- [36] Pollard R J, Murphy A, Hendren W R, Evans P R, Atkinson R, Wurtz G A, Zayats A V and Podolskiy V A 2009 *Phys. Rev. Lett.* **102** 127405
- [37] Wells B M, Zayats A V and Podolskiy V A 2012 *Quantum Electronics and Laser Science Conf. (San Jose, CA, USA, 6–11 May 2012)* **JTh2A.81**
- [38] Orlov A A, Voroshilov P M, Belov P A and Kivshar Y S 2011 *Phys. Rev. B* **84** 045424
- [39] Toscano G, Wubs M, Xiao S, Yan M, Ozturk Z F, Jauho A-P and Asger Mortensen N 2010 Plasmonics: metallic nanostructures and their optical properties VIII ed Stockman M I *Proc. SPIE* **7757** 77571T
- [40] Miano G, Rubinacci G, Tamburrino A and Villone F 2008 *IEEE Trans. Magn.* **44** 822
- [41] Chang R, Chiang H-P, Leung P T and Tse W S 2003 *Opt. Commun.* **225** 353
- [42] de Abajo F J G 2008 *J. Phys. Chem. C* **112** 17983
- [43] Moradi A 2015 *Phys. Plasmas* **22** 032112
- [44] Toscano G, Straubel J, Kwiatkowski A, Rockstuhl C, Evers F, Xu H, Mortensen N A and Wubs M 2015 Resonance shift and spill-out effects in self-consistent hydrodynamic nanoplasmonics *Nat. Commun.* **6** 7132
- [45] Xiang H P, Zhang X, Neuhauser D and Lu G 2014 Size-dependent plasmonic resonances from large-scale quantum simulations *J. Phys. Chem. Lett.* **5** 1163–9
- [46] Kuisma M, Sakko A, Rossi T P, Larsen A H, Enkovaara J, Lehtovaara L and Rantala T T 2015 *Phys. Rev. B* **91** 115431
- [47] Neuhauser D, Pistinner S, Coomar A, Zhang X and Lu G 2011 Dynamic kinetic energy potential for orbital-free density functional theory *J. Chem. Phys.* **134** 144101
- [48] Giannini V, Fernandez-Domínguez A I, Heck S C and Maier S A 2011 Plasmonic nanoantennas: fundamentals and their use in controlling the radiative properties of nanoemitters *Chem. Rev.* **111** 3888
- [49] Haroche S 2013 Controlling photons in a box and exploring the quantum to classical boundary *Rev. Mod. Phys.* **85** 1083–102